

Nanoscale Imaging and Spectroscopy of Plasmonic Modes with the PTIR technique

*Aaron M. Katzenmeyer, Jungseok Chae, Richard Kasica, Glenn Holland, Basudev Lahiri and Andrea Centrone**

Dr. A. M. Katzenmeyer, Dr. J. Chae, R. Kasica, G. Holland, Dr. B. Lahiri and Dr. A. Centrone

Center for Nanoscale Science and Technology, National Institute Standards and Technology, Gaithersburg, 100 Bureau Drive, Maryland 20899, United States

E-mail: andrea.centrone@nist.gov

Dr. J. Chae, Dr. B. Lahiri

Maryland Nanocenter, University of Maryland, College Park, MD 20742 United States.

Keywords: (plasmonics, near-field, PTIR, dark mode, Fano resonances)

The collective oscillation of conduction electrons in plasmonic nanomaterials allows the coupling of propagating light waves with nanoscale volumes of matter (“hot spots”) and allows engineering the optical response of these materials from the UV to THz as a function of nanostructure size and shape. These properties can be leveraged for important applications such as sensing,^[1] photovoltaics,^[2] cloaking^[3] and therapeutics.^[4] For example, plasmonic nanostructures with resonances in the mid-infrared enable surface-enhanced infrared absorption (SEIRA),^[1b, 5] increasing the chemical detection limits of IR spectroscopy up to the zeptomolar range.^[1a] Despite numerous practical applications only a few experimental techniques are available to characterize plasmonic materials with high spatial resolution.^[1b, 6] For example, scattering type scanning near-field optical microscopy (s-SNOM) measures the light scattered by an atomic force microscope (AMF) tip in proximity of a sample and has been successfully used to map the near-field properties of plasmonic structures. However, the limited wavelength tunability of s-SNOM IR sources allowed for the interrogation of plasmonic structures at only one^[7] or a few wavelengths^[6b] or as a convolution of broad-band excitation.^[8] In any case, the spectrum of a plasmonic structure in the near-field has not been reported yet and theoretical calculations are typically necessary to guide experiments, extract

meaningful data,^[9] and put the sparse experimental points into context. On the contrary, by measuring the near-field absorption^[10] (not scattering), the photothermal induced resonance (PTIR)^[1b, 10, 11] technique allows nanoscale resolution imaging and spectroscopy over the whole mid-IR spectral range.^[12] In this work, we apply the PTIR technique to obtain the first near-field absorption spectra of gold asymmetric split ring resonators (ASRRs)^[13] and to image their plasmonic modes. Since the PTIR spectra are not affected by scattered field,^[1b] the absorption properties of plasmonic nanostructures can be obtained without the spectral profile complexities of Fano resonances typically observed in s-SNOM and far-field spectroscopies. With this contribution, we show that in addition to insulators^[12] and semiconductors,^[14] metals are also amenable to PTIR characterization, an important step forward to apply the PTIR technique to a wide variety of functional devices. PTIR^[1b, 10, 11] combines the lateral resolution of atomic force microscopy (AFM) with the chemical specificity of IR absorption spectroscopy, breaking the diffraction limit of IR light and enabling materials identification at the nanoscale by direct comparison with IR spectral libraries.^[15] PTIR uses a tunable pulsed laser for sample illumination and an AFM tip in contact mode as a mechanical detector for extracting local spectral information. PTIR samples are placed or fabricated on an optically transparent prism and are illuminated by total internal reflection to minimize the direct light-tip interaction (Figure 1 a). The absorption of a laser pulse by the sample under the tip causes local heating, sample expansion, and the mechanical excitation of the AFM cantilever. A four-quadrant detector monitors the cantilever deflection as a function of time by measuring the position of the AFM laser reflecting from the cantilever. The local infrared absorption spectrum is obtained by determining the maximum amplitude of the tip deflection (Figure 1 b) as a function of wavelength. PTIR images are obtained by illuminating the sample at a fixed wavelength while scanning the AFM tip.^{[10, 12,}
^{16]} Because of the low laser repetition rate (1 kHz), each new pulse excites the sample and cantilever only after they have returned to equilibrium. A zinc selenide lens is used to focus

the light under the AFM tip while a polarization control module consisting of a set of three mirrors controls the polarization of linearly polarized light at the sample. The typical laser spot size is $\approx 30 \mu\text{m}$, but the AFM tip functions as a “spatial filter” allowing the extraction of spectroscopic information with nanoscale resolution, much smaller than the diffraction limit of IR light.^[10, 11b, 15] PTIR has been applied for nanoscale characterization of bacteria,^[11b, 16] polymers,^[10, 12, 15, 17] metal-organic frameworks,^[18] inorganic particles,^[12, 14] and cells.^[19] Using tunable laser sources with a repetition rate that matches one of the AFM cantilever mechanical resonance self-assembled monolayers could also be measured.^[20] Very recently, the PTIR technique was applied to characterize gold asymmetric split ring resonators arrays^[1b] and quantify the SEIRA enhancement in the near-field for the first time. We named this technique Surface Enhanced PTIR (SE-PTIR).^[1b] However, the PTIR signal intensity, proportional to the linear expansion coefficient (α) and inversely proportional to the thermal conductivity (η) of the sample,^[12, 21] makes the direct measurement of metallic structures (small α and large η) challenging. Previously, to overcome these limitations, the large α of polymer films was exploited to mechanically amplify the PTIR signal of underlying metallic structures and indirectly image their plasmonic modes.^[1b] However, for such a system, the very large SE-PTIR signal due to direct absorption in the polymer layer overwhelms the indirectly measured plasmon absorption when the two spectrally overlap, thus preventing the acquisition of near-field plasmonic spectra and limiting the ability of imaging the plasmonic modes to spectral regions where the polymer absorption is negligible.^[1b] The results presented here show that PTIR can indeed be used to directly interrogate metallic structures, offering improved spatial resolution to map the near-field absorption in these materials. Additionally, PTIR spectra of the plasmonic structures can now be collected directly without the limitations imposed by the spectral overlap with the polymer film. Such investigation was possible due to improved procedures for both alignment of the IR laser and signal optimization (see the Supporting Information experimental information for details). ASRRs^[13] are plasmonic

structures composed of two metallic arcs with a common center. By changing the resonator diameter it is possible to tune the resonator's plasmonic resonances across the whole mid-IR spectral range^[1b] a characteristic that can be exploited for increasing the sensitivity of IR spectroscopy via the SEIRA effect.^[1b, 5] To allow PTIR measurements, the gold resonators arrays were fabricated directly on zinc selenide right angle prisms with a combination of electron beam lithography and lift-off (see supplemental information),^[1b] using custom adaptor pieces described previously.^[10] In this work we study the absorption properties in the near-field of an asymmetric split ring resonators array (hereafter ASRR-1) characterized by resonators with an external diameter of $1900 \text{ nm} \pm 45 \text{ nm}$, a thickness of $100 \text{ nm} \pm 10 \text{ nm}$, and a pitch of $12 \text{ } \mu\text{m} \pm 0.06 \text{ } \mu\text{m}$ as determined by AFM. Another three samples were prepared and characterized in the far-field, namely: an array consisting of the ASRR's left arc only, an array consisting of the ASRR's right arc only, and an ASRRs array (ASRR-ref) used for reference, made by arcs with the same size of the left arc only and right arc only samples. The pitch in these three arrays was $10 \text{ } \mu\text{m} \pm 0.07 \text{ } \mu\text{m}$. The ASRR-ref sample has external diameter of $1790 \text{ nm} \pm 11 \text{ nm}$ and a thickness of $120 \text{ nm} \pm 5 \text{ nm}$. On both ASRR-1 and ASRR-ref, protrusions up to about 50 nm are common at the edges due to non-perfect lift off during fabrication. The uncertainties in the resonator diameter, pitch, and height correspond to a single standard deviation as measured by AFM and arise mostly from the nanofabrication process. The plasmonic response of the resonators is strongly polarization dependent and for linear polarization it is stronger for polarization parallel to the long direction of the arcs, hereafter parallel polarization. All FTIR and PTIR experiments were recorded using light with parallel polarization. It is well known that the plasmonic modes of metallic structures in close proximity couple via near-field interactions and that their resulting optical properties are well described by the plasmon hybridization model.^[22] According to this model the plasmonic resonances of each individual arc in an A-SRR hybridize leading to a lower energy antisymmetric and a higher energy symmetric collective modes.^[1b, 22a] The constructive and

destructive interference of the broader symmetric “bright” mode with the narrower anti-symmetric “dark” mode^[2, 23] generates two maxima and a minimum in the resonators’ far-field reflection spectra (Figure 2). In particular, such interference leads to a Fano-shaped profile which makes plasmonic peaks sharper and increases their Q -factor with respect to their symmetric counterparts due to low scattering losses of the dark-mode.^[23] The interference between the bright and dark mode that generates the Fano distortion, makes the far-field spectral response of the resonators different than the bare sum of the response originating from the individual arcs’ (Figure 2). In contrast with the far-field reflection spectra, no Fano distortion is observed in the PTIR spectra (see Figure 3a) because the PTIR signal is proportional to the product of the optical power density and plasmon absorption coefficient^[1b] while it is independent of scattering. Furthermore, the PTIR technique not only improves the spatial resolution of IR spectroscopy but also greatly improves its sensitivity, even for samples with relatively unfavorable thermo-mechanical properties like gold. For example, the far-field FTIR reflectance spectra of the ASRR-1 array, obtained by averaging the response of approximately 200 resonators (see Figure S1) requires averaging hundreds of spectra to achieve a signal to noise ratio comparable to that obtained by averaging four PTIR spectra which measure the response of a single resonator in the same array (Figure 3a). Importantly, while probed locally, the PTIR spectrum is characteristic of the resonator’s collective plasmonic modes, not of the constituent isolated arc. For example, the spectral intensity of the resonator’s PTIR spectrum is much larger than that of individual arcs, which were not measurable under the experimental condition used in this work, because of the large absorption coefficient due to the resonators’ dark-mode. Finite-element-method calculations suggested^[1b] that under the conditions of PTIR experiments (45° angle illumination) the energy absorbed by the arcs is mostly due to the dark-mode excitation. However, because of their spectral overlap, the bright and dark modes interfere. At longer wavelengths the dark-mode is excited almost exclusively and a larger fraction of the optical power is dissipated by

the longer arc. At shorter wavelengths, the interference of the dark-mode with a small admixture of the bright-mode increases the power dissipated by the short arc and suppresses the power dissipated by the long one. In between, the energy dissipated in each arc changes as a result of the interference of the two modes. The PTIR images (Figure 3 b–f) display the energy dissipated within the arcs due to the plasmonic excitation^[24] providing evidence of the interference between the two modes. The PTIR spectra (Figure 3a) identify the cross over between the energy density dissipated in the two arcs at $7.2 \mu\text{m}$ (1384 cm^{-1}). Based on this local spectroscopic information a shift from dissipation predominantly in the shorter right arc at shorter wavelengths to dissipation predominantly in the longer left arc for longer wavelengths is expected. Such behavior is clearly supported by the PTIR maps in Figure 3 b–f (displayed in full scale). For example, at shorter wavelengths (1472 cm^{-1} , Figure 3b and 1432 cm^{-1} , Figure 3c), the dissipation is primarily localized in the shorter right arc. As expected, at 1384 cm^{-1} (Figure 3d) both arcs are equally excited. At longer wavelengths, (1268 cm^{-1} , Figure 3e and 1184 cm^{-1} , Figure 3f) the dissipation occurs predominantly in the longer left arc. The same maps are plotted in common intensity scale after normalization with respect to incident laser power in the supplemental information (Figure S2). Such images show that the stronger absorption occurs at $\approx 1268 \text{ cm}^{-1}$ and that it is localized predominantly in the longer left arc which is consistent with the PTIR spectra (Figure 3a). Such spectra represent an important step forward in IR plasmonic research as they not only confirm the prediction of previous finite-element calculations^[1b] but also offer standalone experimental guidance for imaging plasmonic modes in the near-field.

Overcoming the need of a polymeric mechanical amplification layer and measuring the resonators directly allows resolving the mode structure of the plasmonic excitation better which could be beneficial to understand the role of fabrication defects in the resonator's response. For example, PTIR maps in reference^[1b] revealed subtle differences in the response of one ASRR with respect to another. We can now directly observe potential causes of such

differences. See the left arc in Figure 3c and the right arc in Figure 3 e in relation to the height image in Figure 3a (inset). The edge roughness resulting from the liftoff procedure contributes to local variation of signal intensity which may be expected to result in subtle differences in the resonators' response. Another benefit of mapping the plasmonic modes directly is the improved spatial resolution. For example, Figure 3f shows that the heating due to the plasmon excitation is strongest at the arc tips where the electric field is maximum. This type of excitation resembles the dipolar excitation observed in gold nanorods^[7a] and may be speculatively attributed to a relatively localized thermal excitation. The comparison of height and PTIR line profiles (Figure S3) reveals that the PTIR mapping resolution is limited by the pixel size to ≈ 30 nm, an order of magnitude smaller than the arcs width. In contrast, the PTIR lateral resolution obtained when imaging the resonators' plasmonic modes coated by a polymer layer was limited by heat diffusion in the polymer layer to a value comparable with the polymer layer thickness (≈ 200 nm).^[1b] We believe that by measuring absorbed and scattered light respectively, PTIR and s-SNOM are complementary techniques for studying the near-field properties of materials. For example, the bright mode and the dark mode of plasmonic structures behave differently: the bright mode excitation results predominantly in scattered light and in little absorption while for the dark-mode the scattered light is much weaker and the absorbed light is strong.^[1b] In contrast, the detection mechanism of s-SNOM makes this technique typically more sensitive to the scattered light. More specifically, the scattered light detected in s-SNOM experiments is a complex function of tip-sample near-field interactions, the sample's local index of refraction, and the local absorption coefficient which necessitates nontrivial theoretical modelling to attempt the reconstruction of IR absorption spectra from the data. While such complexity if disentangled may provide a wealth of information about the sample's near-surface region, the simpler PTIR approach has several important characteristics which make its data immediately informative. Namely: (i) the topographic and the spectral information are acquired at different timescales preventing any

crosstalk between the two channels,^[1b] (ii) the PTIR spectra are a measure of sample absorption and can be used as is for materials identification via direct comparison with IR spectral databases,^[15] (iii) the PTIR signal increases linearly with sample thickness up to $\approx 1 \mu\text{m}$,^[10] enabling nanoscale quantitative analysis. These characteristics, combined with the broad tunability of PTIR laser sources^[12, 25] make the PTIR technique a very useful tool for characterizing materials at the nanoscale. In conclusion we applied the PTIR technique to directly characterize individual plasmonic nanostructures in the near-field with both high spectral and spatial resolution. This approach enabled the extraction of the first local near-field plasmonic IR absorption spectra, which are free of Fano-distortions. In particular, local PTIR spectra of A-SRRs predict well the crossover in the absorbed energy localization from short arc to long arc with increasing wavelength as a result of the interference between bright and dark modes. Such spectra provide guidance to map the energy dissipated in the resonators at wavelengths of interest without necessitating theoretical calculations. Here it is shown that in addition to insulators^[12] and semiconductors^[14] metals can also be measured with the PTIR technique, an important step forward in applying this characterization method to a variety of state-of-the-art functional devices (e.g. flexible electronics or nanocomposites) which synergistically combine diverse materials to engineer novel functionality.

Experimental Section

FTIR Spectroscopy: Fourier Transform Infrared (FTIR) spectra were recorded at near normal incidence with an FTIR spectrometer equipped with an infrared microscope by illuminating the entire array with a 36x reverse Cassegrain reflection objective (NA = 0.52) and a ZnSe wire grid polarizer (to control the light polarization). 512 spectra (4 cm^{-1} resolution) were acquired and averaged for each sample.

PTIR Experimental set up: PTIR experiments were carried out using a commercial PTIR setup which consists of an AFM microscope operating in contact mode and a tunable pulsed laser

source consisting of an Optical Parametric Oscillator (OPO) based on a non-critically phase-matched ZnGeP₂ crystal. The laser emits pulses 10 ns long at 1 kHz repetition rate which are tunable from 4000 cm⁻¹ to \approx 1025 cm⁻¹ (from 2.5 μ m to 9.76 μ m). The samples on a ZnSe prism were illuminated by total internal reflection (Figure. 1a) focusing the laser light under the AFM tip with a ZnSe lens. The typical spot size is 30 μ m \pm 10 μ m depending on the wavelength. The laser output is linearly polarized and a rotating ZnSe wire grid linear polarizer is used as a variable attenuator to control the light intensity. A polarization control module, consisting of three motorized mirrors, is used to obtain the desired polarization at the sample. Most of the optics in the PTIR setup and inside the laser are placed on motorized stages which allow automatic wavelength selection and sweeping via a computer interface. Since different wavelengths are typically emitted by the OPO at different angles, an infrared pyroelectric camera was used to calibrate the mirror positions resulting in the laser output co-linearity in the entire wavelength range.

PTIR experiments: PTIR spectra were obtained by averaging the cantilever deflection amplitude from 256 individual laser pulses at each wavelength and tuning the laser at intervals of 4 cm⁻¹. Four consecutive spectra were averaged to increase the signal to noise ratio. PTIR images were recorded by illuminating the sample at constant wavelength while scanning the AFM tip in contact mode. The AFM height and the PTIR signal acquisition was synchronized so that for each AFM pixel the PTIR signal is an average over a fixed number of laser pulses^[10] (64 in this work). The pixel sizes are 30 nm x 30 nm in all images. All PTIR experiments were recorded with linearly, s-polarized light with the electric field vector always in the resonators plane and parallel to the long direction of the arcs. Commercially available 450 μ m long silicon contact-mode AFM probes with a nominal spring constant between 0.07 N/m and 0.4 N/m were used for this study.

Supporting Information

Supporting Information is available from the Wiley Online Library or from the author.

Acknowledgements

J. C. and B. L. acknowledge support under the Cooperative Research Agreement between the University of Maryland and the National Institute of Standards and Technology Center for Nanoscale Science and Technology, Award 70NANB10H193, through the University of Maryland.

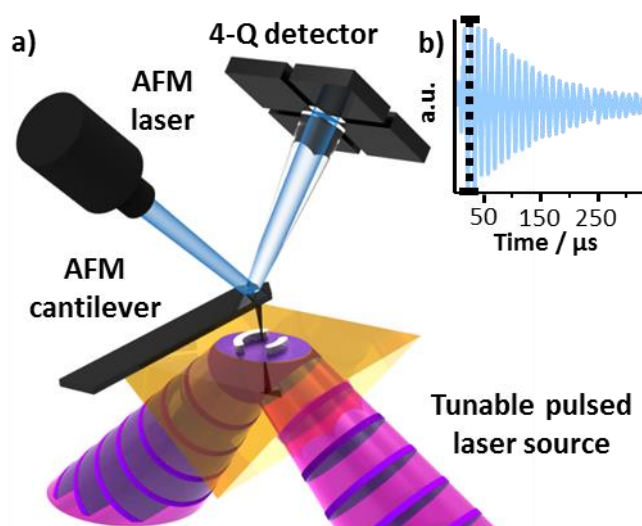


Figure 1. a) Schematic of the PTIR measure: The pulsed IR laser beam (purple discs within the pink envelope) illuminates the sample via total internal reflection. The absorption of a laser pulse in the sample causes the sample to thermally expand and deflects the AFM cantilever proportionally to the absorbed energy. The cantilever deflection is measured with a four-quadrant detector that monitors the position of the AFM laser reflecting from the AFM cantilever. b) PTIR deflection signal as a function of time. The maximum amplitude of the tip deflection was used to obtain PTIR maps and spectra.

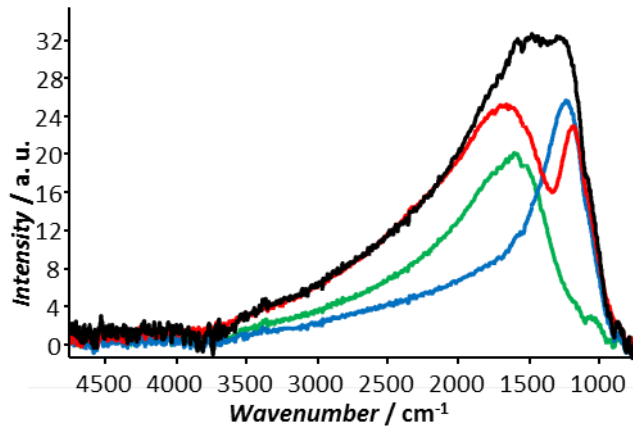


Figure 2. Far-field FTIR reflection spectra for: ASRR-ref array (red), left arcs only array (LA, blue), right arcs only array (RA, green), and calculated intensity sum of the individual arcs (LA+RA) arrays (black).

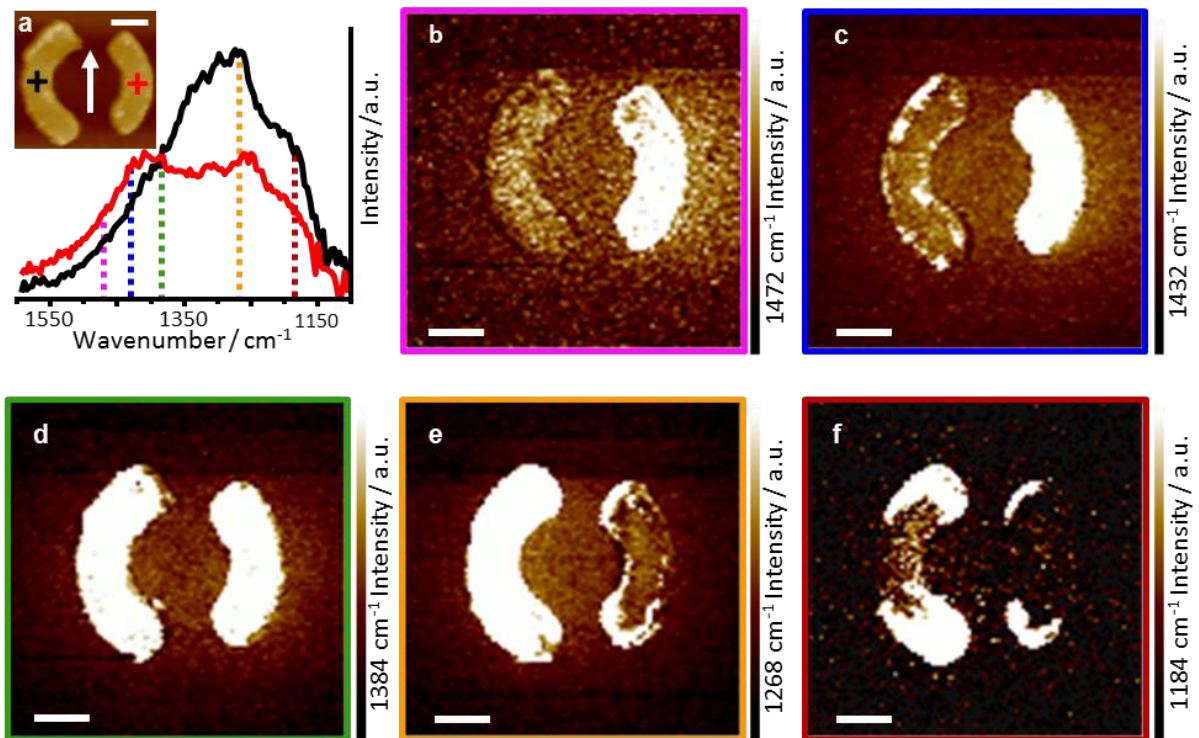


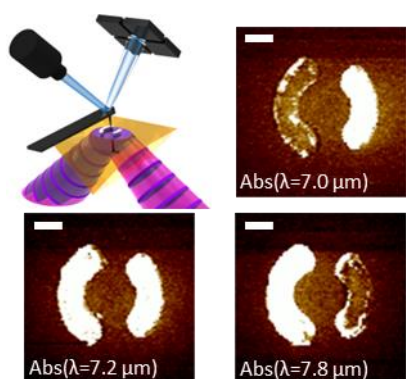
Figure 3. **a)** PTIR spectra of the ASRR-1 sample collected at locations identified by a color coded “+” in the inset height image. **b,c,d,e,f)** PTIR maps (each displayed with its own, unique full scale) emphasize the contribution of each arc to the collective modes of the resonator at several wavelengths of interest (identified by dotted color coded vertical lines in fig. 3a). All scale bars are 500 nm: the white arrow in the height inset indicates the direction of the electric field polarization in the PTIR experiments.

The photothermal induced resonance (PTIR) method measures the near-field absorption in gold plasmonic structures. PTIR absorption images show the interference between the bright and dark modes of asymmetric split ring resonators (A-SRRs). The plasmonic absorption spectra of the ASRR's individual arcs are obtained locally confirming the collective nature of the plasmonic excitation. Scale bars are 500 nm.

Keyword

Dr. A. M. Katzenmeyer, Dr. J. Chae, R. Kasica, G. Holland, Dr. B. Lahiri and Dr. A. Centrone*

Nanoscale Imaging and Spectroscopy of Plasmonic Modes with the PTIR technique



Copyright WILEY-VCH Verlag GmbH & Co. KGaA, 69469 Weinheim, Germany, 2013.

Supporting Information

Nanoscale Imaging and Spectroscopy of Plasmonic Modes with the PTIR technique

*Aaron M. Katzenmeyer, Jungseok Chae, Richard Kasica, Glenn Holland, Basudev Lahiri and Andrea Centrone**

Supplemental experimental information:

Alignment of the PTIR laser: The alignment of the IR laser under the AFM tip requires iterative adjustment of the laser focus (z), and position (x,y) for multiple wavelengths. This is carried out initially with a graphitic sample that absorbs across the mid-IR wavelength region and used as reference. We refer to this procedure as the instrument alignment calibration. For any sample of interest the iterative adjustment of the laser focus (z), and position (x,y) for multiple wavelengths is performed again to align the laser under the tip to account for variability in the focus position due to different light path lengths in the prism as a function of the specific sample position on the prism top surface. Typically this procedure is carried out initially with a relatively strong power to obtain a first measurable signal. Later, the signal is maximized by iteratively tightening the focus spot and moving its position under the AFM tip. As the laser focus spot tightens typically the laser power is reduced to avoid damaging the sample. However the alignment of the IR laser under the AFM tip for the samples studied in this work is challenging because the resonator structures can be easily damaged and delaminated by the laser and because the response of the resonators is not homogeneous (i.e. the response of the right arc is quite different than for the left arc). To overcome these difficulties we performed an additional alignment on a reference sample containing poly-methyl methacrylate (PMMA) particles placed on the same x,y position as the resonators but a on a different prism. This alignment was used to obtain coarse settings to start the final fine alignment on the resonator sample which required only small corrections in x,y,z for each

wavelength. The laser alignment was validated for at multiple points on the resonator structure for several wavelengths.” Laser pulse energy was reduced as necessary throughout the process to prevent resonators damage which can occur with as little as 1.4 μJ for tightly focused beams at strongly resonant wavelengths.

Sample Fabrication: All chemicals were used as received without further purification. A-SRRs arrays were fabricated directly on ZnSe prisms. The prisms were cleaned in an ultrasonic bath with acetone (1 min) and methanol (1 min). A bilayer of PMMA positive electron beam resist was spun (25 Hz) on top of the prism, using a custom adaptor piece described previously.^[S1] The resist was heated (140 °C for 30 min) before depositing an aluminum charge dissipation layer (30 nm \pm 5 nm) with an electron-beam evaporator. The A-SRRs square arrays 250 μm x 250 μm were written on the ZnSe prisms using an electron beam lithography custom-made adaptor.^[S1] The accelerating voltage was 100 kV and the electron beam dose was 1000 $\mu\text{C}/\text{cm}^2$ (A-SRR-ref) or 1600 $\mu\text{C}/\text{cm}^2$ (ASRR-1). The aluminum layer was then removed using an aqueous tetramethylammonium hydroxide (2.4 % volume fraction) solution. The pattern was developed in a mixture of Methyl Iso-butylketone (MIBK) and isopropyl alcohol (IPA). Electron beam deposition was used to deposit (0.1 nm/s at $6.67 \cdot 10^{-4}$ Pa) a thin chromium adhesion layer (\approx 5 nm) and a gold layer [100 nm \pm 10 nm (ASRR-1), 120 nm \pm 5 nm (ASRR-ref)]. Finally, the A-SRRs arrays were obtained after liftoff in hot N-methylpyrrolidone remover (45 °C).

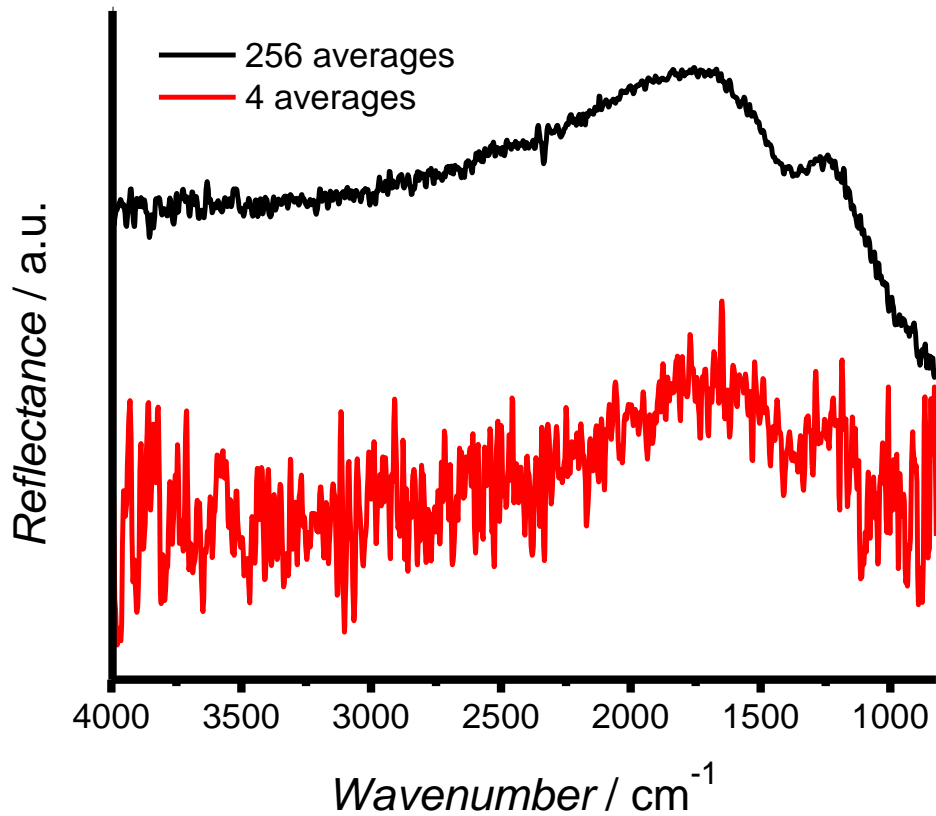


Figure S1. Far-field FTIR reflectance spectra of ASRR-1 sample collected from an area containing ≈ 200 resonators. The red spectrum is the average of 4 spectra (the same number of spectra averaged in the PTIR spectra in figure 3 of the main text). Despite recording the signal from hundreds of A-SRR structures, 256 spectra must be averaged (black spectrum) to obtain a signal to noise ratio comparable to that obtained in the PTIR spectrum of a single resonator (obtained by averaging just 4 spectra).

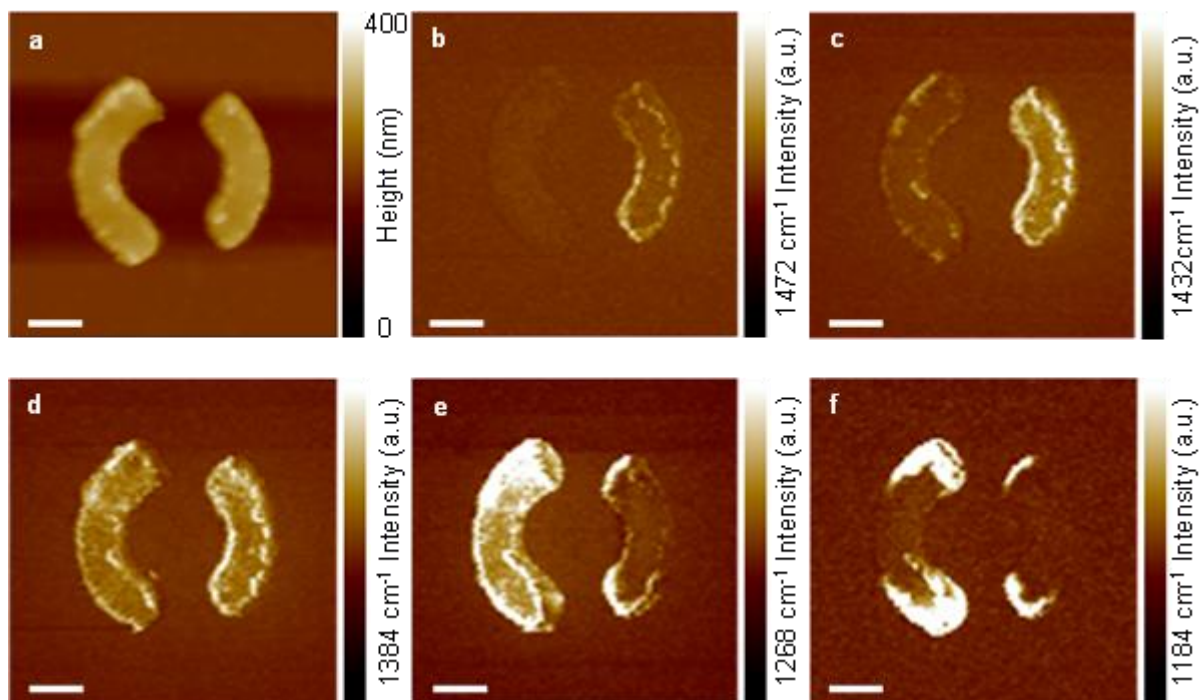


Figure S2. AFM height image and PTIR maps (plotted in common scale, normalized with respect to incident laser power) for the A-SRR reported in figure 3 of the main text. Scale bars are 500 nm; the white arrow in the height inset indicates the direction of the electric field polarization in the PTIR experiments.

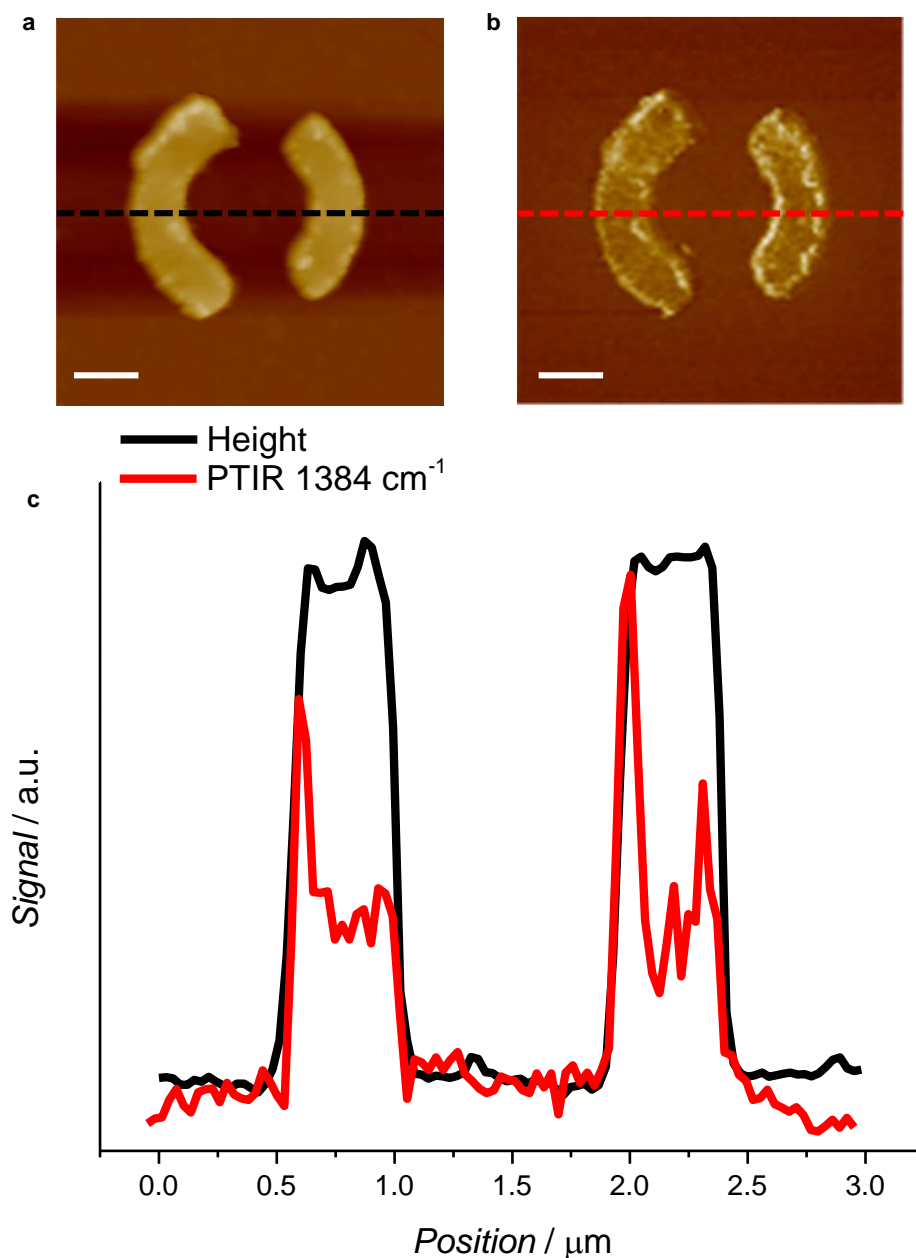


Figure S3. a) Height and b) PTIR (at 1384 cm⁻¹) images of the ASRR-1 sample. Scale bars are 500 nm. c) Line profiles of height and PTIR signals along the dashed lines in the height and PTIR images, respectively. The PTIR lateral resolution is comparable to the resolution of the height image and is limited to 30 nm by the pixel size.

Supporting References

[S1] B. Lahiri, G. Holland, A. Centrone, *Small* **2013**, 9, 439.